

## Supplementary Materials for

### **Peripheral membrane proteins modulate stress tolerance by safeguarding cellulose synthases**

Christopher Kesten *et al.*

Corresponding author: Miguel A. Botella, [mabotella@uma.es](mailto:mabotella@uma.es); Clara Sánchez-Rodríguez, [clara\\_sanchez@ethz.ch](mailto:clara_sanchez@ethz.ch)

*Sci. Adv.* **8**, eabq6971 (2022)  
DOI: 10.1126/sciadv.abq6971

#### **The PDF file includes:**

Figs. S1 to S8  
Table S1  
Legend for movie S1

#### **Other Supplementary Material for this manuscript includes the following:**

Movie S1

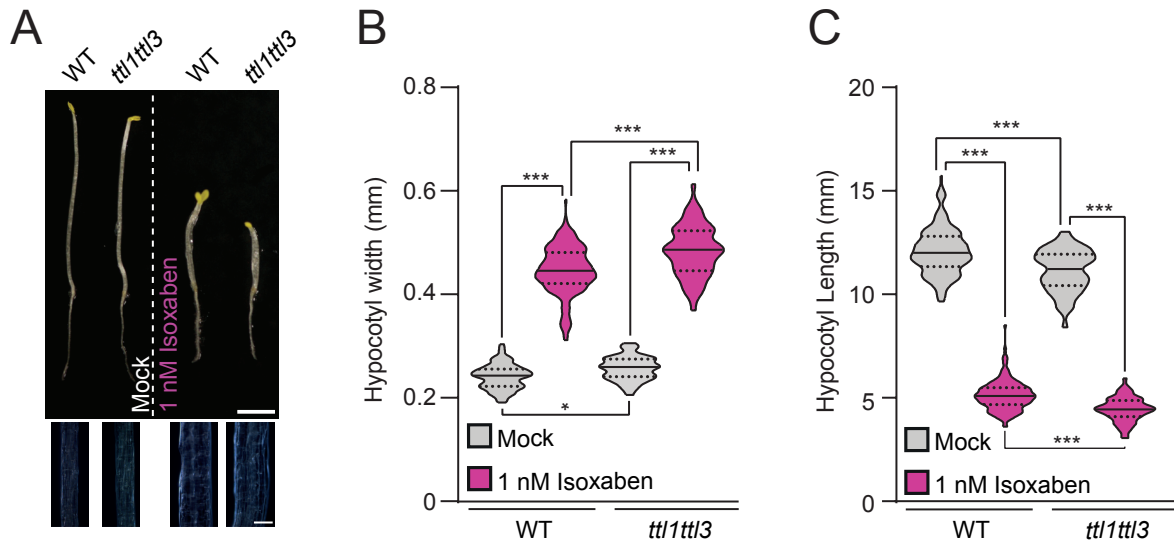


**Fig. S1. *tt1ttl3* seedlings show increased sensitivity to isoxaben.**

(A) 5-day-old etiolated WT (Col-0) and *tt1ttl3* seedlings germinated on control or media supplemented with 1 nM isoxaben (upper panels). Magnifications show distinctive hypocotyl width in *tt1ttl3* double mutant plants in 1nM isoxaben, indicative of defective anisotropic growth (lower panels). Scale bar=5 mm (upper image) and 200  $\mu$ m (close-up hypocotyls). (B) and (C) Quantification of hypocotyl width (B) and length (C) of seedlings as depicted in (A). Violin plots: centerlines show the medians; dotted lines indicate the 25th and 75th percentiles;  $N \geq 11$  seedlings from 3 independent experiments. Unpaired t-test; \* $p$ -value $\leq 0.05$ , \*\* $p$ -value $\leq 0.01$ , \*\*\* $p$ -value $\leq 0.001$ .

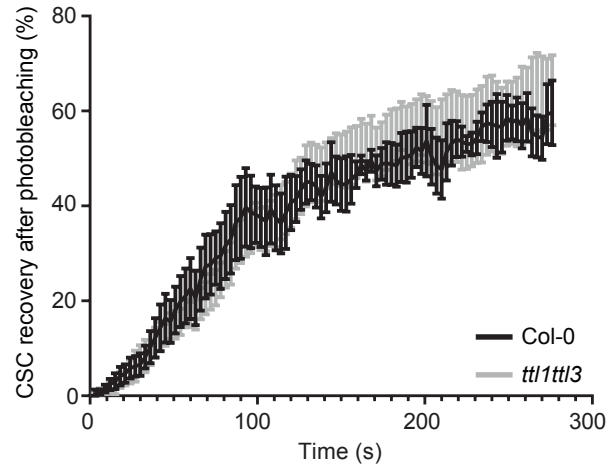


**Fig. S2. *ttl1ttl3* mutant is not affected in CESA delivery to the plasma membrane.**

Fluorescence Recovery After Photobleaching (FRAP) of 3-day-old WT (Col-0) and *ttl1ttl3* etiolated hypocotyl epidermal cells expressing YFP-CESA6. Graph displays re-population of the plasma membrane at indicated time points with fluorescent CESA foci as percentage of CESA density at  $t=0$  (just before FRAP). Two-way ANOVA analysis of CESA recovery;  $p=0.84$  (genotype),  $p\leq 0.001$  (time),  $p>0.99$  (genotype  $\times$  time).  $N\geq 7$  cells from at least five seedlings and three independent experiments. Values are mean $\pm$ SEM.

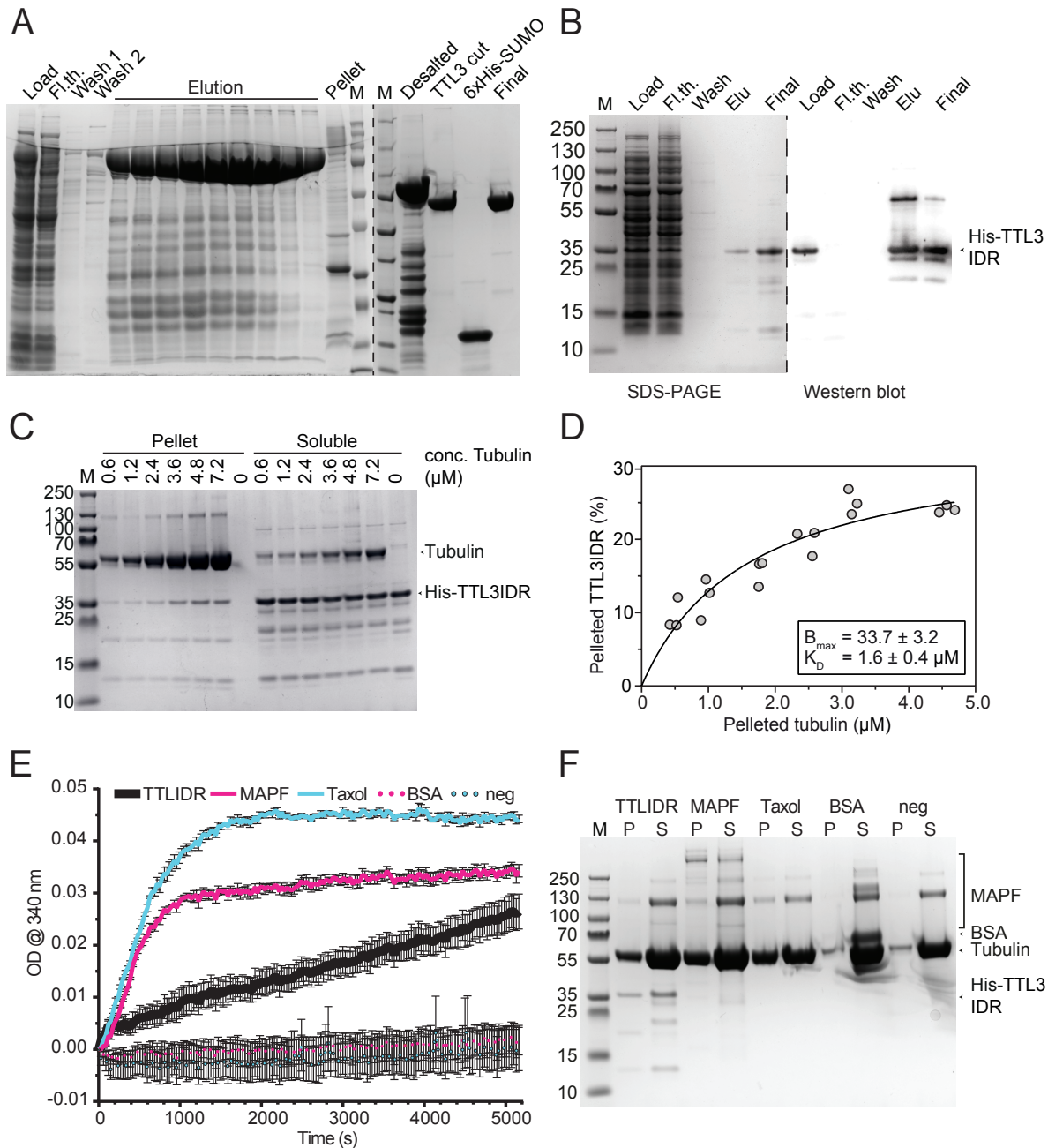


**Fig. S3. TTL3IDR interacts with and promotes microtubule formation.**

(A) Expression and purification of 6xHis-SUMO-TTL3. SDS-PAGE gel of the purification steps. M = Molecular marker; Load = crude protein extract; Fl.th. = flowthrough after Ni-NTA Agarose binding; TTL3 cut = TTL3 after digestion with SUMO protease and gel filtration; Final = Desalted, cut and concentrated protein. (B) Expression and purification of 6xHis-TTL3IDR. Left panel: Coomassie-stained SDS-PAGE gel of the purification steps. M = Molecular marker; Load = crude protein extract; Fl.th. = flowthrough after Ni-NTA Agarose binding; Elu = Imidazole elution; Final = Desalted and concentrated protein. Right panel: Representative image of a Western blot to detect 6xHis-TTL3IDR. (C) Representative Coomassie gel used to estimate the dissociation constant for 6xHis-TTL3IDR and microtubules. Tubulin and 6xHis-TTL3IDR molecular sizes are indicated by

arrowheads. **(D)** The binding affinity of 6xHis-TTL3IDR to microtubules was determined by calculating their dissociation constant ( $K_D$ ) ( $1.6 \pm 0.4 \mu\text{M}$ ; best-fit values  $\pm$  Std. Error). 6xHis-TTL3IDR levels were kept constant while the amount of microtubules was increased.  $K_D$  was calculated by fitting a saturation binding curve onto the data, obtained from images as in (F);  $N=3$  independent experiments. **(E)** Microtubule turbidity assay. Tubulin was incubated with buffer (neg) or BSA as negative controls, a microtubule-associated protein fraction (MAPF) or taxol as positive controls, and the 6xHis-TTL3IDR. Microtubule formation was measured at 340 nm. Values are mean  $\pm$  SEM.  $N=3$  technical replicates. **(F)** Reactions, as shown in (C), were spun down, separated in pellet and supernatant fractions, and analyzed by SDS-PAGE. While distinct tubulin bands at 55 kDa are visible in the pellet fraction of the positive controls (MAPF, taxol) and 6xHis-TTL3IDR, indicative of microtubule formation and tubulin stabilization, clear smearing of bands appears in the supernatant fractions of the negative controls (BSA, buffer), indicative of no microtubule formation and tubulin degradation. M = Molecular marker; P = Pellet fraction; S = Supernatant fraction.

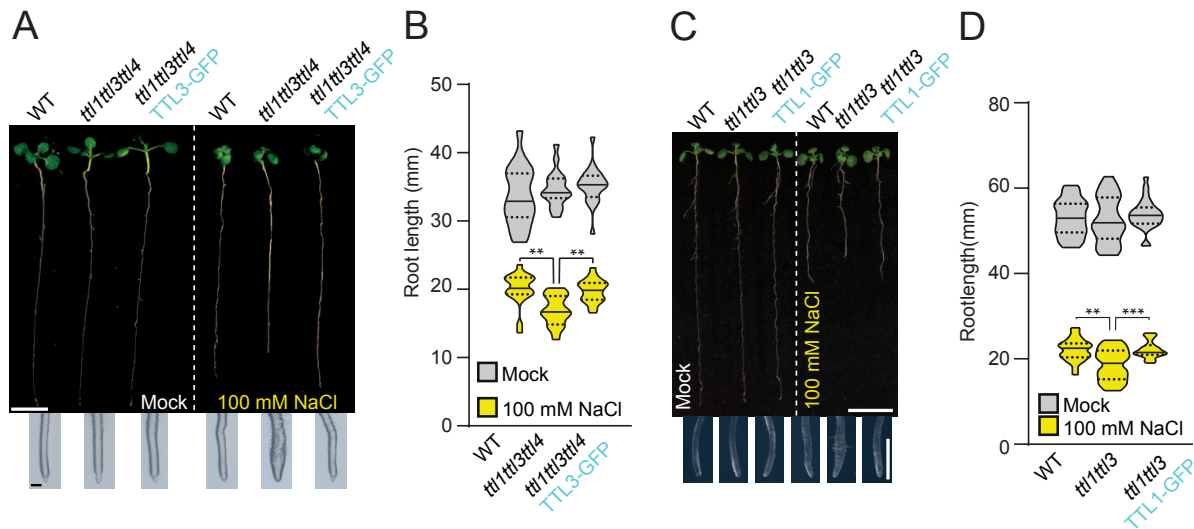


**Fig. S4. *TLL3-GFP* and *TLL1-GFP* driven by their own promoters complement the root growth defects of *ttl* mutants in the presence of NaCl.**

(A) The *TLL3-GFP* construct complements the root growth defects of the *ttl1ttl3ttl4* mutant seedlings on NaCl. 3-day-old WT (Col-0), *ttl1ttl3ttl4*, and *ttl1ttl3ttl4* *TLL3-GFP* seedlings germinated and grown on control conditions were transferred to control and NaCl containing media and grown in the light for 8 additional days (upper panels). Magnifications show distinctive root tip swelling in *ttl1ttl3ttl4* triple mutant plants under salt stress, indicative of anisotropic growth failures (lower panels). Scale bars=5 mm (upper image) and 200  $\mu$ m (close-up root tips). (B) Quantification of root length of seedlings as in (A). Violin plots: centerlines show the medians; dotted lines indicate the 25th and 75th percentiles; Welch's ANOVA between mock groups:  $p$ -value=0.29; Welch's ANOVA between NaCl treated groups:  $p$ -value $\leq$ 0.001; Dunnett's T3 multiple comparison: \*\* $p$ -value $\leq$ 0.01.  $N\geq$ 15 roots and three independent experiments. (C) The *TLL1-GFP* construct complements the root growth defects of the *ttl1ttl3* mutant seedlings on NaCl. 3-day-old WT (Col-0), *ttl1ttl3*, and *ttl1ttl3* *TLL1-GFP* seedlings germinated and grown on control conditions were transferred to control and NaCl containing media and grown in the light for 8 additional days (upper panels). Magnifications show distinctive root tip swelling in *ttl1ttl3* triple mutant plants under salt stress, indicative of anisotropic growth failures (lower panels). Scale bars=1 cm (upper image) and 1 mm (close-up root tips)  $\mu$ m. (D) Quantification of root length of seedlings as in (C). Violin plots: centerlines show the medians; dotted lines indicate the 25th and 75th percentiles; Welch's ANOVA between mock groups:  $p$ -value=0.29; Welch's ANOVA between NaCl treated groups:  $p$ -value $\leq$ 0.001; Dunnett's T3 multiple comparison: \*\* $p$ -value $\leq$ 0.01, \*\*\* $p$ -value $\leq$ 0.001.  $N\geq$ 15 roots and two independent experiments.

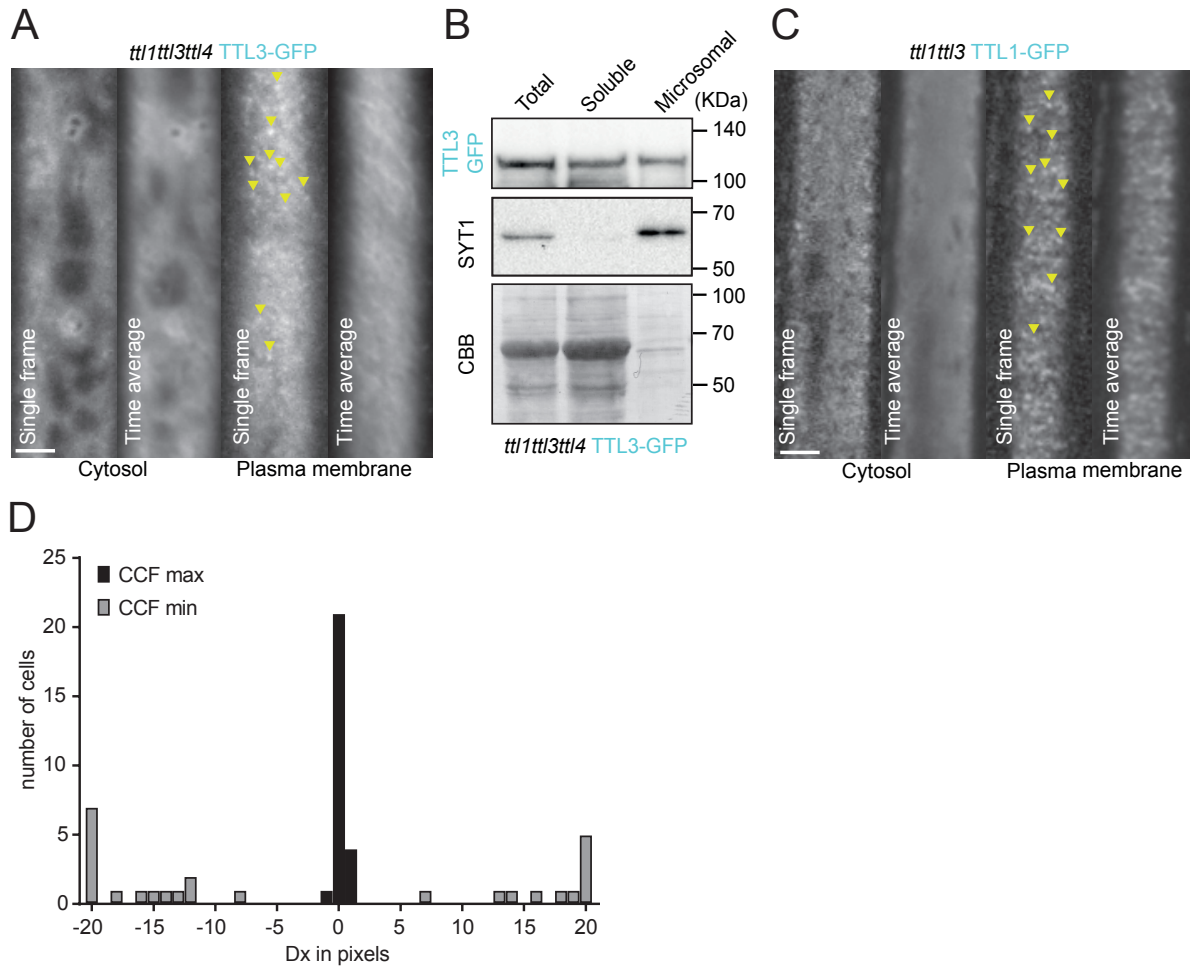


**Fig. S5. TTL1 and TTL3 are peripheral membrane proteins that co-migrate with the Cellulose Synthase Complex.**

(A) TTL3-GFP in 3-day-old etiolated hypocotyl epidermal cells of *ttl1ttl3ttl4* TTL3-GFP seedlings. TTL3-GFP signal is visible as cytosolic signal and as distinctive motile particles (yellow arrows) at the plasma membrane as revealed by single frames and time-average projections. Scale bar=2.5  $\mu$ m. (B) Fractionation analysis (total, soluble, and microsomal fractions) of TTL3-GFP in *ttl1ttl3ttl4* as in (A). TTL3-GFP and the microsomal control SYT1 were detected with an anti-GFP and anti-SYT1 antibodies, respectively. Coomassie brilliant blue (CBB) staining provides a loading control. The experiment was repeated 3 times with similar results. (C) TTL1-GFP in 3-day-old root epidermal cells of *ttl1ttl3* TTL1-GFP seedlings. TTL1-GFP signal is visible as cytosolic signal and as distinctive motile particles (yellow arrows) at the plasma membrane as revealed by single frames and time-average projections. Scale bar=2.5  $\mu$ m. (D) Quantification of TTL3-GFP and tdT-C6 co-localization in hypocotyl cells of three-day-old etiolated seedlings. Cross-correlation coefficients (CCFs) were calculated in the original non-shifted images (dx = 0) and after being shifted with dx  $\pm$  20 pixels using the van Steensel's algorithm. Note the highest CCFs (CCF max, black bar) were detected at dx = 0 for n = 21 cells. Gray bars represent the shifts that lead to the lowest CCF (CCF min), where the overlap of signals was the lowest.

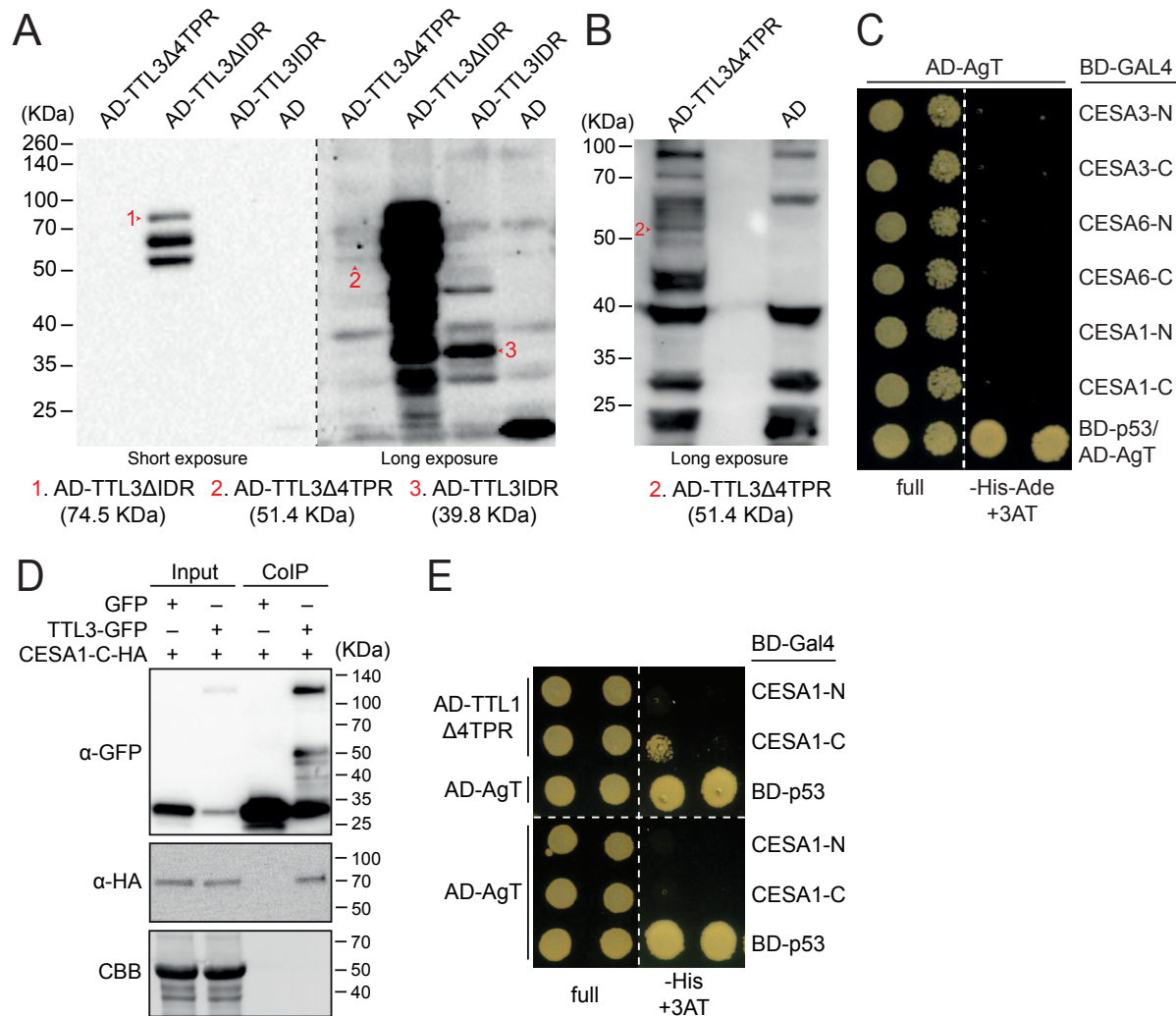


**Fig. S6. Yeast-2-hybrid constructs used in the study are expressed and do not auto-activate. TTL1 interacts with CESAs in a similar way as TTL3.**

(A) Immunoblot analysis showing the expression of AD-TTL3ΔIDR, AD-TTL3Δ4TPR, and AD-TTL3IDR in protein extracts of yeast transformants used for the yeast-two-hybrid assays. For each of them, yeast transformants were resolved in polyacrylamide/SDS-Page gels and analyzed by immunoblot using an anti-HA Tag monoclonal antibody. The expected molecular size of (1) AD-TTL3ΔIDR, (2) AD-TTL3Δ4TPR, and (3) AD-TTL3IDR is represented in the figure. (B) Immunoblot analysis showing the expression of AD-TTL3Δ4TPR and AD in protein extracts of yeast transformants used for the yeast-two-hybrid assays. Representative Western-blot of independent AD-TTL3Δ4TPR and AD yeast transformants of those shown in (A) Western blot was performed as described in Fig.S6A. (C) Negative control of yeast-two-hybrid assays of the cytosolic CESA-N and CESA-C BD domains with BD-GAL4. BD-p53/AD-AgT was used as a positive control of the interaction. Growth on non-selective media (full) and interaction-selective media (lacking histidine and adenine [-His-Ade] and supplemented with 3-amino-1,2,4-triazole [+3AT]) are shown. Photographs were taken after 3 days. Three independent experiments yielded similar results. (D) TTL3-GFP was transiently co-expressed with CESA1-C-HA or free GFP as a negative control in *N. benthamiana*. Total (Input) and co-immunoprecipitated (CoIP) proteins were analyzed by immunoblotting using anti-GFP and anti-HA antibodies. Equal loading was confirmed



by Coomassie blue staining (CBB) of input samples. Two independent experiments yielded similar results. **(E)** Yeast-two-hybrid assays showing the interaction of TTL1 $\Delta$ 4TPR (amino acids 1 to 307) with CESA1-C. Growth on non-selective media (full) and interaction-selective media (lacking histidine [-His] and supplemented with 3-amino-1,2,4-triazole [+3AT]) are shown. Photographs were taken after 3 days. A positive control (BD-p53/AD-AgT) for the yeast two-hybrid assays is shown. -N=N-terminal region of CESAs; -C=catalytic cytosolic loop of CESAs. The experiment was repeated 3 times with the same results.



**Fig. S7. *ttl1ttl3* exacerbates the *prc1-1* developmental defects.**

Morphological phenotypes of 5-week-old plants of WT (Col-0), *ttl1ttl3*, *prc1-1*, and *ttl1ttl3prc1-1* grown in long-day conditions. Scale bar=1 cm.

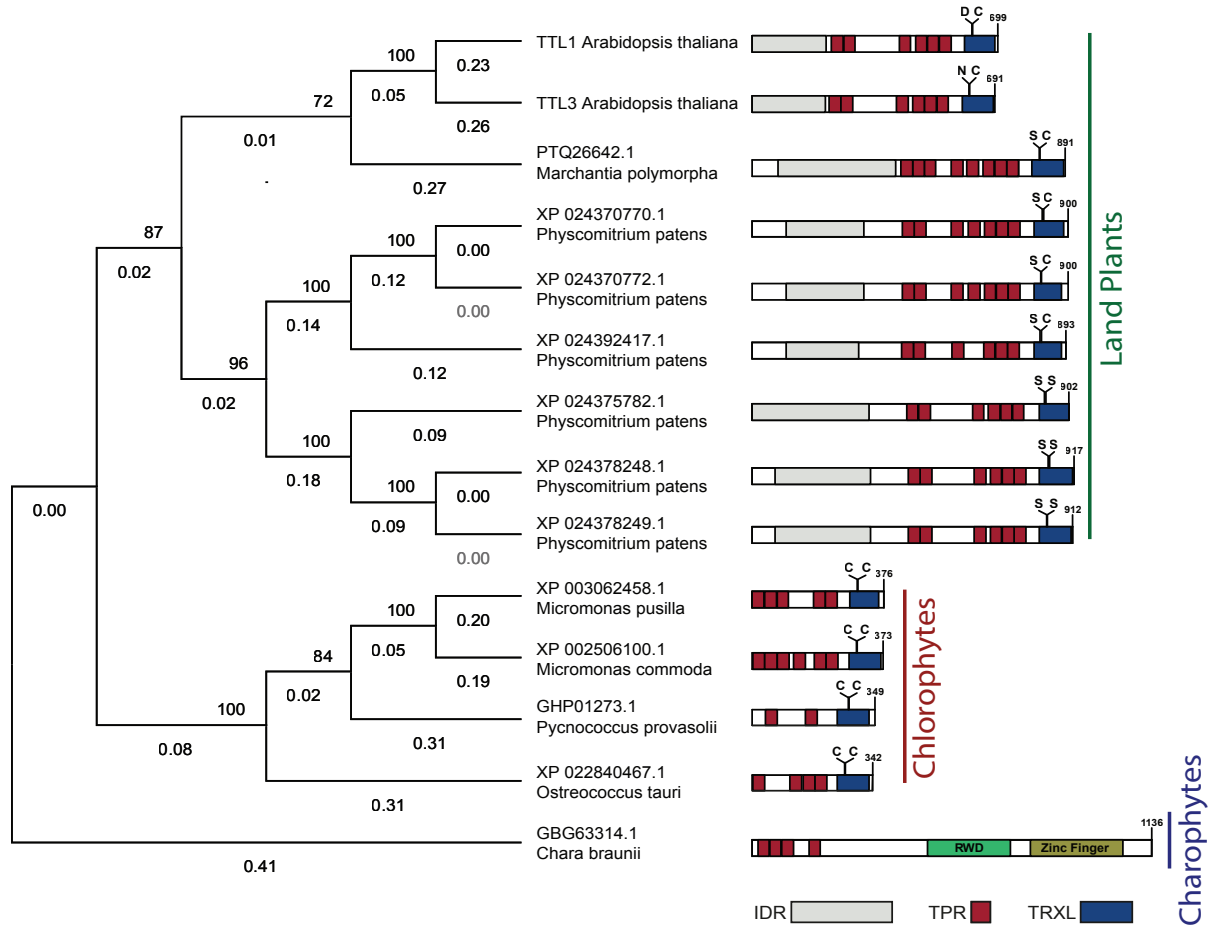


**Fig. S8. TTL genes have emerged in land plants.**

Identification of Arabidopsis TTL1 and TTL3 orthologs in Embryophytes (earliest land plants), Chlorophyta, and Charophytes. The earliest TTL orthologs can only be identified in Embryophytes. IDR = intrinsically disordered region; TPR = tetratricopeptide repeat; TRX = C-terminal sequence with homology to thioredoxins and conserving the essential Cys residues required for thioredoxin activity; TRXL = TRX domain lacking essential Cys residues conserved for thioredoxin activity. Bootstrap test (0-100): 500 replicates; evolutionary distances: *p*-distance (0-1).

**Table S1. Primers used in this study**

Description	Forward	Reverse
TTL1 dPCR	TGGACTCACCACCACCACTA (LP)	ACCGAGTCTGCGAACAAGAT (RP)
TTL3 dPCR	AGAGAGCTGCGATGCTTGAT (LP)	ATGCTCTCTCCACATCCAC (RP)
TTL4 dPCR	AATGAACCATTAAATTGGGGC (RP)	ATGTGAAGAATGTGGCGAAAG (LP)
CESA1-C in pDONR/Zeo	AAAAAGCAGGCTCCATGGATCAGTTCCCAA ATGGTAC	AGAAAGCTGGGTCGGTGTGATATAAGCG ATCCTCTC
pTTL1::TTL1g in pENTR	CACCACAAATTCGTTTCGTACACGGT	ACCGCTATAGTGTCTCACCG
TTL3IDR in pDONR/Zeo	TAGAAGGGTGGGCGCGCCGAC	TCCTCCGCCGTGCGTAC
TTL3IDR ColonyPCR	CTGGTAAACCGTCGGTGAGT	GGGATATCAGCTGGATGGCAAA
SALK dPCR (LBb1.3)	ATTTTGCCGATTTCCGGAAC	
SAIL dPCR (LB3)	TAGCATCTGAATTTCCATAACCAATCTCGATACAC	
Cesa1-N-Y2H	GACCTGCATATGATGGAGGCCAGTGCC	ATTCGGCCTCCATGGCCTTAGCGAGAAGATG GGATAGG
Cesa1-C-Y2H	GACCTGCATATGATGGATCAGTTCCCAAAT GGTACC	TCGGCCTCCATGGCCTTAGGTGTTGATATAA GCGATCCTC
Cesa3-N-Y2H	GACCTGCATATGATGGAATCCGAAGGAGAA ACC	ATCGGCCTCCATGGCCTTACATTCTGTAAGG ATTGATCCG
Cesa3-C-Y2H	GACCTGCATATGATGGATCAGTTCCCAAAT GGTTTC	ATTCGGCCTCCATGGCCTTAGGTGGTGTTCAC ATACGC
Cesa6-N-Y2H	GACCTGCATATGATGAACACCGGTGGTCG	TCGGCCTCCATGGCCTTACATCCGTAAGGA TTTATCTTG
Cesa6-C-Y2H	GACCTGCATATGATGGATCAGTTCCCTAAAT GGTACC	ATTCGGCCTCCATGGCCTTAAGAGGTCCACG GGTAAAC
TTL3IDR in pPROEX HTb	AGGGCGCCATGGGATCCGGAATGTCGCATTC CCGTCGC	CCTCGAGACTGCAGGCTCTAGATCACGCTTT CCCAGAGGTACCG
TTL3 in petM11SUMO3GFP	GTTCCAGCAACAGACCGGTGGATCCATGTCT CATTCTAGAAGACTTTCGTTGGA	CTCGCCCTTGCTCACGGATCCTCATAAGAGG AAATGCTTATAGAGTCTCTAG

**Caption for Movie S1**

TTL3-GFP particles co-localize with tdT-CesA6 at the plasma membrane (see merged image series). TTL3-GFP image series are shown non-modified (non-mod) and after extracting particles at the plasma membrane with an image modification pipeline (mod).